JOURNAL OF Materials CHEMISTRY

Infrared and *in situ* ^{119}Sn Mössbauer study of lithiated tin borate glasses

C. Gejke,*[a] E. Nordström,[b] L. Fransson,[c] K. Edström,[c] L. Häggström[b] and L. Börjesson[a]

[a]*Department of Applied Physics, Chalmers University of Technology, S-412 96 Göteborg, Sweden. E-mail: gejke@fy.chalmers.se; Fax: +46 31 7722090; Tel: +46 31 7725175*
[b]*Department of Physics, Uppsala University, S-751 21 Uppsala, Sweden*
[c]*Department of Materials Chemistry, Uppsala University, S-751 21 Uppsala, Sweden*

Received 9th April 2002, Accepted 24th June 2002
First published as an Advance Article on the web 9th August 2002

The effect of lithium ion insertion/extraction in a SnB_2O_4 glass electrode, particularly how it affects the glass network structure and the tin environment, has been investigated using *in situ* Mössbauer and diffuse reflectance infrared (DR-IR) spectroscopy. Two different potential ranges for the electrochemical cycle were investigated; (0.01–0.8) V and (0.01–1.0) V. During the first cycle of both potential ranges the lithium ions first inserted in to the electrode are observed to cause substantial disruption to the glass network. This disruption to the glass network appears to cause a large (50%) irreversible capacity loss in the first cycle. We also demonstrated differences in the cycling stability for different voltage ranges. The (0.01–0.8) V range showed superior cycling stability with a capacity of around 530 mA h g^{-1} for at least 25 cycles. The *in situ* Mössbauer and DR-IR results show that during the subsequent 25 cycles the glass structure undergoes mainly reversible changes for both the potential ranges. However, the Mössbauer spectra of electrodes cycled in the (0.01–1.0) V range indicate a continuous change in the tin environment towards a more symmetric and lithium rich one for the fully charged state after 25 cycles, which is not observed for cycling in the (0.01–0.8) V range. This may explain the lower capacity experienced for cells cycled in the (0.01–1.0) V range.

Introduction

Rechargeable lithium ion batteries are now used in many everyday applications as cellular phones, camcorders and laptop computers. The usefulness of these batteries has boosted extensive activity in the development of new and improved materials for batteries with higher capacity, superior chemical and mechanical stability, higher safety and improved cycleability. In the search for new materials, a research group from Fuji Film Co. Ltd., has suggested a tin-based amorphous composite oxide (TCO), which shows twice the gravimetry and even four times the volumetric capacity of the carbon-based material used today.[1] The outstanding performance regarding the lithium ion storage capacity of the TCO glasses developed so far is counterbalanced by the large ($\sim$50%) irreversible capacity arising during the very first cycle. The cause of this detrimental effect is not yet fully understood and neither is the lithium ion insertion/extraction process. A mechanism has been suggested[2] where lithium ions are believed to react irreversibly with SnO forming Li_2O and metallic Sn. Thereafter a reversible alloy formation between Sn and Li-ions is supposed to take place with $Li_{4.4}Sn$ as the end product. In this model the glass network is regarded to consist of only spectator atoms that do not influence the cycling process. Recently, however, results have been reported that indicate the host glass network has a significant role in the lithium insertion/extraction process.[3–8] Techniques such as NMR, EXAFS, Mössbauer, IR[3–12] have been used to study the changes of the lithium and tin environment as well as the host glass structure during the lithium insertion/extraction process. The actual behaviour of the glass structure has been difficult to interpret since the pristine glass structure is not known and neither is the initial environment of the tin.

The original TCO glass ($SnB_{0.56}P_{0.40}Al_{0.42}O_{3.6}$) has a complex composition with many different glass forming oxides beside the electrochemically active SnO. In order to clarify the importance of each component during the cycling process, simplified variants of the TCO glasses have recently been synthesised using a fewer number of oxides. Some of the less complicated TCO glasses studied so far are Sn_2BPO_6, $Sn_2P_2O_7$ and $Sn_2B_2O_5$.[2,4,7] The structure and chemical composition of the glass forming oxides has then been found to be of high significance for the lithium ion insertion/extraction process. In this study we have performed infrared reflectance and *in situ* Mössbauer experiments on a SnB_2O_4 glass together with some additional Mössbauer measurements on a $Sn_2B_3O_{6.5}$ glass. The aim of this study is to determine the structural changes that occur in the glass network as well as in the tin environment during electrochemical cycling.

Experimental

The SnB_2O_4 and $Sn_2B_3O_{6.5}$ glasses were made by mixing appropriate amounts of SnO and B_2O_3. The ground mixtures were heated in a graphite crucible under an Ar atmosphere to 1000 °C for at least 6 hours. The mixtures were then quenched onto a copper plate at room temperature. The amorphous state was confirmed using X-ray diffraction. An ICP (inductively coupled plasma) analysis was performed on the glass as to ensure the ratio between tin and boron.

The electrodes were made out of ground glass material, Shewinigan black, and a polymer binder PVDF [poly(vinylidene fluoride)] on a copper current collector (18 μm) with a mass ratio of 82 : 10 : 8. A total loading of approximately 10 mg per electrode was achieved with an electrode area of 3.14 cm^2. A thin foil of metallic lithium (125 μm) was used as the counter electrode and the electrolyte consisted of a 1 M solution of $LiPF_6$ (Merck) in ethylene carbonate–dimethyl carbonate (2 : 1 by volume; Selectipur®, Merck, Darmstadt Germany). The electrochemical cells were sealed in polymer laminated aluminium bags in an argon filled glove-box (O_2,

H_2O <2 ppm). Details of the electrode and cell preparation have been reported previously.[7] The cells were discharged and charged potentiostatically on a MacPileII^{TM} to different potentials and thereafter allowed to reach electrochemical equilibrium prior to the measurements. The extended cell cycling was performed on a Digatron BTS-600 battery tester in galvanostatic mode with a current density of 0.1 mA cm^{-2}. Cells were cycled between either 0.01 and 0.8 V or 0.01 and 1.0 V.

Diffuse reflectance infrared (DR-IR) spectra were collected using a Bruker IFS 66v/S FT-IR spectrometer equipped with a DTGS detector using a diffuse reflectance device (Graseby Specac, mod. Selector). The resolution was 4 cm^{-1} and 200 scans were accumulated for each spectrum. Finely grained KBr-powder was used as reference. The data were treated by taking the ratio of the reflected intensity from the electrode to that from the reference and converting the result using the Kubelka–Munk procedure.[13]

The electrochemical cells were examined *in situ* using Mössbauer spectroscopy at appropriate potentials during both charge and discharge processes in the first electrochemical cycle. A couple of cells were also investigated after 25 cycles of repeated charge–discharge to study the stability of the glass-material during further cycling. A sample of pure glass powder was measured too after it had been mixed with boron nitride and pressed into a disc. The spectra were recorded in transmission geometry using a conventional constant acceleration vibrator (Wissel MR-360). A 3 mCi $Ca^{119m}SnO_3$ source was used with a proportional counter (Outokumpu 490) as the detector. Acceptable statistics were achieved in approximately a week for a typical spectrum because of the low amount of active material on the electrodes. In order to calibrate the velocity scale, spectra for α-Fe were recorded simultaneously on the opposite side of the vibrator.

Results and discussion

Electrochemical cycling

Electrodes were cycled between two different potential ranges, (0.01–0.8) V and (0.01–1.0) V. In Fig. 1 the capacity *vs.* cycle number is displayed for the two different potential ranges. It is seen that the main capacity loss occurs during the first cycle independent of the potential range. However, the Fig. 1 clearly shows that the potential range strongly affects the cycling stability and that the potential range (0.01–0.8) V gives superior long term cycling capacity. The better stability in the (0.01–0.8) V range was also seen from a comparison of the Faradaic loss between the 2nd and the 25th cycle. The loss was only 3% for the (0.01–0.8) V range compared to 23% for the (0.01–1.0) V range.

Behaviour of the glass network structure during cycling; infrared spectroscopy

When adding another metal oxide to a borate glass, the boron atoms continuously change their coordination from three-fold to four-fold until about one oxygen to each boron has been added.[14,15] On further addition of oxide, the coordination of the boron atoms changes back to three-fold but now with partly non-bridging oxygens. The amount of SnO present in SnB_2O_4 suggests that the glass network should be a mixture of three- and four-coordinated borons with one non-bridging oxygen per BO_3 unit. The stretching vibrational bands associated with four-coordinated boron units are to be found between 800 cm^{-1} and 1200 cm^{-1}, and those with three-coordinated boron units appear between 1200 cm^{-1} and 1550 cm^{-1}.[16] In the DR-IR spectra of the uncycled electrode in Fig. 2a, a major band centred at 1460 cm^{-1} and a smaller one at about 1110 cm^{-1} could be detected. Hence there are bands present in both the regions related to three- and four-coordinated borons, supporting the structural model mentioned above. The spectrum also shows a band at 715 cm^{-1} that is attributed to the bending of B–O–B bonds.[16]

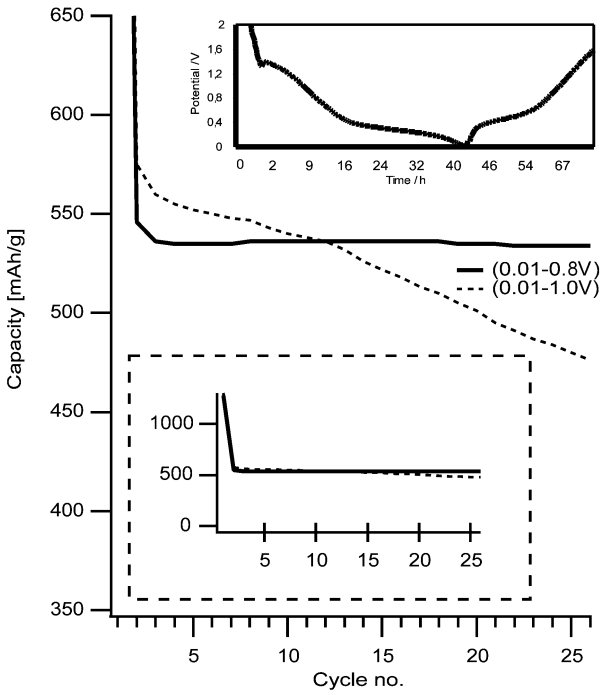

Fig. 1 Capacity curves for the SnB_2O_4 electrodes for different voltage ranges. At the top right corner, the first cycle for the glass electrode is shown.

From Fig. 2a it can be seen that after full discharge to 0.01 V during the first cycle, large changes in the IR spectra are evident. The strong band at 1460 cm^{-1} is now shifted to around 1350 cm^{-1} and a new band at 790 cm^{-1} appears. The peak at 1350 cm^{-1} is usually assigned to the B–O asymmetric stretch in units where the boron atoms are three-coordinated to oxygen (BO_3 units). The inserted lithium ions interfere with the BO_3 units and thereby give rise to distorted B–O bonds. The band at around 790 cm^{-1} can be assigned to the bending of $^{-}O–B–O^{-}$ bonds, *e.g.* in smaller borate units as pyroborate ($B_2O_5^{4-}$) groups. From the fully discharged state up to 0.8 V only small changes occur within the glass network. The most prominent change is the appearance of a shoulder at 1410 cm^{-1}, probably due to pyroborates.[16] When charging to 1.5 V, the peak at 1460 cm^{-1} is regained and the peak at 1350 cm^{-1} is diminished indicating a partly reversible interaction between lithium ions and some of the borate units. The band at 715 cm^{-1} disappears during the cycling and is substituted with a band at 790 cm^{-1}. Since the band at 715 cm^{-1} is not recovered on charging to 1.5 V, as noticed in Fig. 2a, irreversible structural changes take place that involve disruption of the B–O–B bonds, *i.e.* bonds between the borate units have been broken. This disruption can also be seen from the presence of some typical bands for pyroborate at 660, 1115 and 1410 cm^{-1}.[16] It is also possible that shorter borate units, *i.e.* orthoborates, are formed as reported in previous studies.[7,8] However, pyroborate ($B_2O_5^{4-}$) and orthoborate (BO_3^{3-}) both exhibit bands that overlap each other at around 1260 cm^{-1} and 760 cm^{-1} and because of this, the presence of orthoborate is thus difficult to probe. The formation of lithium orthoborate[7,8] as well as pyroborate during the first discharge cycle suggests that they are a major contributing factor to the irreversible capacity loss that occurs during the first cycle. Other factors that might influence the amount of irreversible capacity are for the moment not known. The effects of electrolyte decomposition *etc.* are regarded as being negligible compared to the glass disruption.

DR-IR spectra of cells cycled 25 times, taken at 0.8 V and

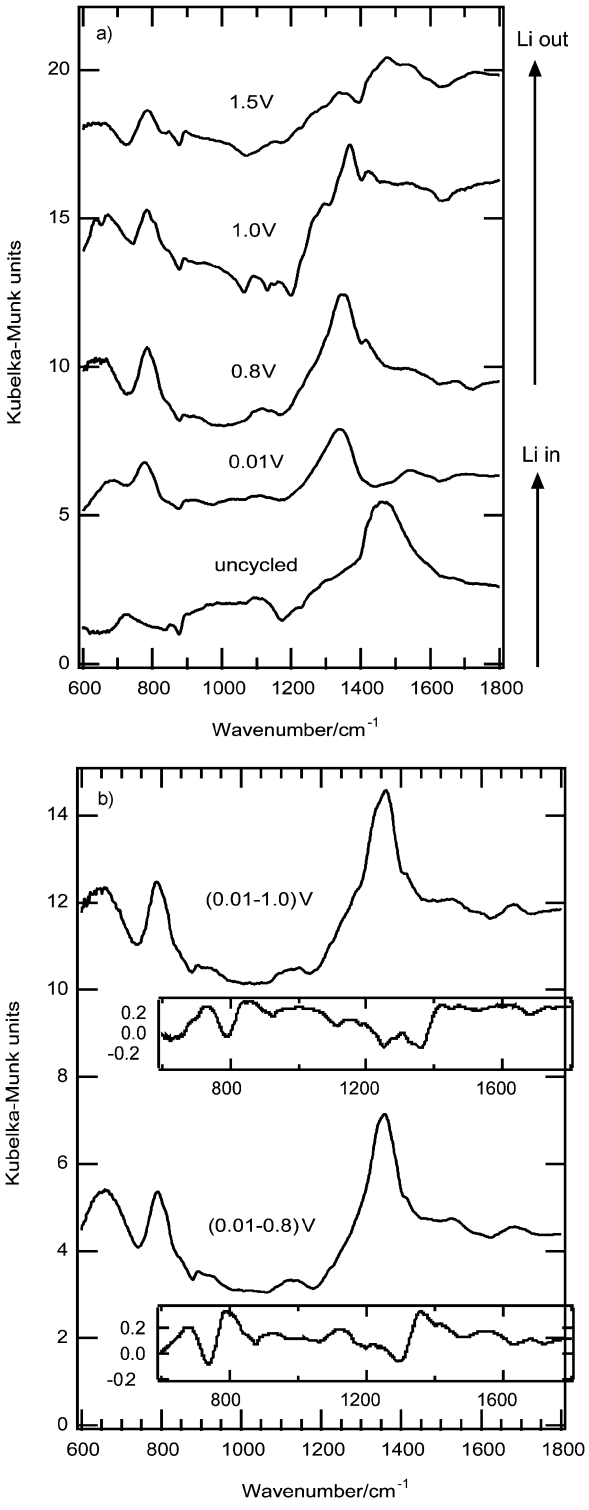

Fig. 2 a) DR-IR spectra of SnB_2O_4 electrodes at different stages during the first cycle. The spectrum at 1.0 V has additional bands arising from the electrolyte. b) DR-IR spectra of SnB_2O_4 electrodes after the 25th cycle for the different voltage ranges. In the insets, the difference between the 1st and 25th cycle are shown.

1.0 V depending on the potential-range, are displayed in Fig. 2b. The structural difference between the electrodes cycled in the potential ranges (0.01–0.8) V and (0.01–1.0) V is minimal, suggesting that the differences in cycling stability is not due to the glass network. A comparison between spectra taken at the first and at the 25th cycle show only minor differences for both potential ranges. This suggests that the glass network is stable throughout the cycling and that the formation of pyroborate and orthoborate is not dependent on the number of cycles but rather a reaction that takes place during the first cycle.

Behaviour of the Sn environment during cycling; Mössbauer spectroscopy

In Fig. 3, the Mössbauer spectrum of the pure SnB_2O_4 glass is displayed. The spectrum consists of an asymmetric quadrupole split doublet with an isomer shift of about 3.1 mm s^{-1} (all isomer shifts are given versus $CaSnO_3$ at room temperature). The spectrum is similar to spectra recorded previously for some different tin borate glasses.[17] The asymmetry of the doublet can not be explained by the Goldanskii–Karyagin effect[18] since a spectrum recorded with a γ-ray incidence angle of 54.7° to the absorbance plane has exactly the same appearance.[19] Instead a good fit can be obtained using a minimum of three different symmetric doublets, for which each could be assigned to different positions of tin in the glass. The lorentzian linewidth W at full width half maximum (FWHM) obtained from the fit is 0.78 mm s^{-1}, which is only 0.14 mm s^{-1} larger than the natural linewidth. This indicates that the atomic surroundings for each of the three tin positions are very similar since the experimental broadening due to the experimental set up is measured to be around 0.10 mm s^{-1} (from the calibration measurement). The isomer shifts, electric quadrupole splittings and relative intensities of the different sites are (3.17 mm s^{-1}, 1.75 mm s^{-1}, 42%), (3.09 mm s^{-1}, 2.41 mm s^{-1}, 42%) and (3.31 mm s^{-1}, 1.16 mm s^{-1}, 16%) respectively. In general the ^{119}Sn isomer shift is almost linearly dependent on the number of s electrons at the Sn site, *i.e.* a loss in s electrons lowers the isomer shift, while the electric quadrupole splitting mainly emanates from the imbalance in the occupation of the different p_x-, p_y- and p_z-electrons at the Sn site.[20] In our case the three tin positions have rather similar isomer shifts but differ more in the electric quadrupole splittings, which indicates differences in symmetries of the atomic surroundings. If there had been clusters of SnO_2 formed during the glass synthesis, an absorption peak at around 0 mm s^{-1} would have been discerned. However, there is no evidence for SnO_2 cluster formation in this spectrum and hence we can conclude that there is no tin with a valence state Sn^{4+} in the glass.

The Mössbauer spectra for the discharge–charge of the cell are shown in Fig. 4. As opposed to the infrared study the Mössbauer spectra follow the discharge process stepwise. All spectra (except for that at "0.2 V") show a broad symmetric feature without any resolution. The centre of gravity, the broadening and the intensity of the resonance change however from spectrum to spectrum. The fit has therefore to be concentrated to these three features in order to get any reliable

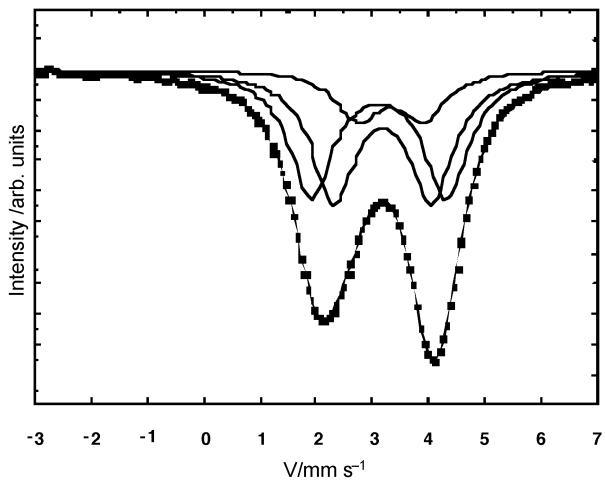

Fig. 3 Mössbauer spectra of the SnB_2O_4 glass consisting of three different subspectras representing various tin sites.

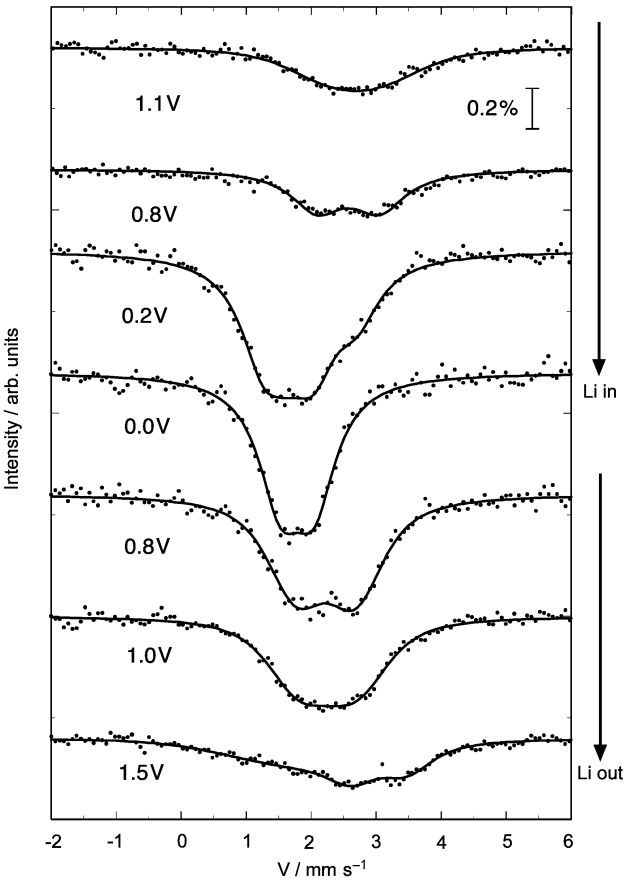

Fig. 4 *In situ* Mössbauer spectra of the SnB_2O_4 cell during the first cycle.

data from these poorly resolved spectra. The centre of gravity of a symmetric spectrum gives the average isomer shift while the broadening gives the average value of the electric quadrupole splitting and its standard deviation. Finally, the intensity tells us something about the Mössbauer recoil free factor *f*. All spectra were therefore fitted by a model with one isomer shift and one quadrupole splitting with a gaussian distribution. The individual lorentzian linewidths were kept constant in the fitting at 0.78 mm s^{-1}, corresponding to the result from the pristine sample. The results of these fits are given in Table 1. After discharge down to 1.1 V there is almost no signal from the glass structure left, instead the isomer shift has dropped to approximately 2.7 mm s^{-1}. Furthermore the absorption has decreased significantly. Since metallic β-tin has a much lower recoil-free factor than most other tin compounds and an isomer shift of 2.54 mm s^{-1},[21] this could be an indication that metallic tin has formed. However, the spectrum has a quadrupole splitting of about 0.8 mm s^{-1}, which is larger than the value of 0.43 mm s^{-1} reported for β-tin.[22] SnO, which also has a relatively low *f* factor, has a similar value for the isomer shift but a large quadrupole splitting in the order of 1.3–1.8 mm s^{-1}.[23] The present results can thus be interpreted as an aggregation of tin slightly distorted by a close neighbourhood of oxygen atoms. It is also notable that there is no indication of any Sn^{4+} in these spectra since there are no resonances at 0 mm s^{-1}.

Table 1 The hyperfine parameters used to fit the Mössbauer spectra for the SnB_2O_4 cell

Potential/V	δ^a/mm s^{-1}	$<\Delta E_Q>^b$mm s^{-1}	σ^cmm s^{-1}
1.1	2.69 ± 0.05	0.81 ± 0.05	0.8
0.8	2.58 ± 0.05	0.98 ± 0.05	0.6
0.2	1.80 ± 0.05	0.79 ± 0.05	0.6
0.0	1.78 ± 0.05	0.46 ± 0.05	0.0
0.8	2.23 ± 0.05	0.90 ± 0.05	0.3
1.0	2.26 ± 0.05	0.85 ± 0.05	0.5
1.5	2.56 ± 0.05	0.19 ± 0.05	1.9
0 ↔ 0.8 × 25	2.27 ± 0.05	0.86 ± 0.05	0.4
0 ↔ 1.0 × 7	2.23 ± 0.05	0.96 ± 0.05	0.5
0 ↔ 1.0 × 25	2.16 ± 0.05	0.11 ± 0.05	0.8

[a]δ is the isomer shift. [b]$<\Delta E_Q>$ is the average quadrupole splitting. [c]σ the standard deviation of the quadrupole splitting.

After further discharge of the cell it is seen that the 0.8 V spectrum is similar to the 1.1 V spectrum. However, differences, such as a slight decrease in isomer shift and somewhat narrower lines making the spectrum more distinct and β-tin like, can be noticed. This is in agreement with previous results from Mössbauer and NMR spectroscopy,[6,9,12] where formation of β-tin was observed after the insertion of approximately two lithium ions. After further discharge to 0.2 V, the absorption has increased again and the peak is shifted towards lower values even more. This is an indication that there are lithium ions very close to the tin or even that lithium ions have started to alloy with the tin. There is however no perfect match with any of the known alloys of the lithium–tin systems. It is thus plausible that alloy formation occurs continuously and not stepwise and therefore that different alloy compositions are present at the same time. Another important factor is that at this stage only a few lithium and tin atoms are kept together, thus no long-range order exists as for regular alloys. The proximity of oxygen might also explain the divergence from known alloys.[6]

At the fully discharged state for the cell, there is only a single peak present with an isomer shift of 1.8 mm s^{-1}. This spectrum resembles spectra previously ascribed to $Li_{4.4}Sn$.[24] After recharging to 0.8 V the spectrum reveals a doublet with an isomer shift of approximately 2.2 mm s^{-1} and a quadrupole split of 0.90 mm s^{-1}. Thus, according to these values around one or two lithium ions are still alloyed with the tin. After further charge up to 1.0 V, not much has happened to the spectrum except for a slight broadening of the peaks. This would indicate that the structure remains the same only slightly more disordered. Trying to charge the cell further results in a very broad peak at around 2.6 mm s^{-1} with low absorption, indicating a disordered mix of β-tin and SnO_x, and thus a removal of the alloy-like relationship between lithium and tin.

The first cycle is summarised in Fig. 5, where the isomer shift and quadrupole splittings at the different potentials for the SnB_2O_4 cell are compared to the corresponding values for SnO and different alloys of tin and lithium. As seen in the figure, the hyperfine parameters for the cell differ from the parameters reported for crystalline Li_xSn_y alloys although they are in the same range. This deviation might be explained as mentioned above by a difference in the alloy character between lithium and tin but also the presence of nearby oxygen.

The spectra from cells recorded at 0.8 V and 1.0 V for increasing cycle numbers can be seen in Fig. 6. The spectrum for the cell cycled 25 times with 0.8 V as the cut-off potential looks very similar to the spectrum recorded after the first cycle. The spectrum for the cell cycled to 1.0 V has not changed much after the 7th cycle. However, after 25 cycles, the isomer shift has decreased and the quadrupole splitting is less pronounced. The trend observed from previous Mössbauer studies of Li–Sn compounds is that a smaller isomer shift signifies a higher lithium ion content.[24,25] This indicates that more and more lithium ions are trapped in the Li_xSn_y alloy for each cycle in the 1.0 V case. A decrease in the quadrupole splitting suggests that tin is sensing a more symmetric environment. Therefore the changes in the isomer shift and quadrupole splitting indicates that there is a slight increase of lithium near tin and that this lithium surrounds tin in a highly symmetric way. This might even indicate a more ordered structure of the ambient borate units. A schematic picture of the structural changes leading to a more symmetric tin environment is shown in Fig. 7. The change

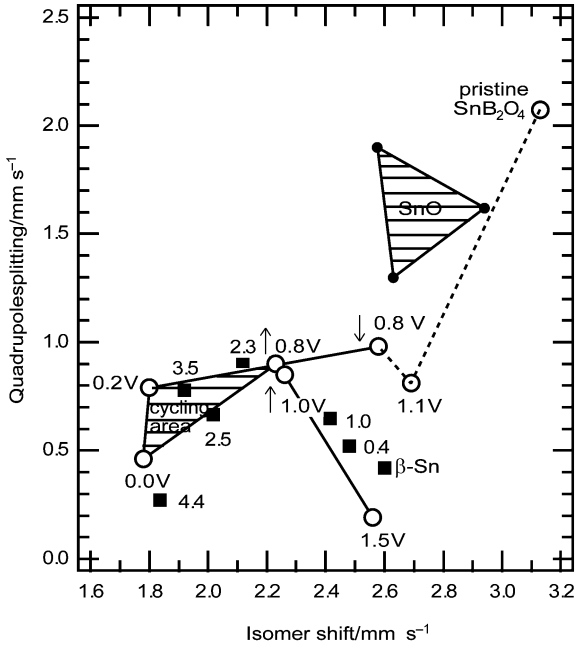

Fig. 5 Plot of electric quadrupole splittings and isomer shifts for the SnB_2O_4 cell at different electric potentials during the first cycle (open dots). The dotted line is the initial glass disruption route. Also shown are the corresponding values for amorphous and crystalline SnO from Isidorsson *et al.*[23] (inside the triangles) and for crystalline compounds of type Li_xSn (average values) from Dunlap *et al.*[24] (black squares).

from an amorphous lithium borate group towards a more crystalline-like group would only affect the infrared vibrations slightly, *i.e.* they would be hardly noticeable in the IR measurements. A slight ordering of a network constituent (phosphate) upon extended cycling has been observed in previous studies.[6]

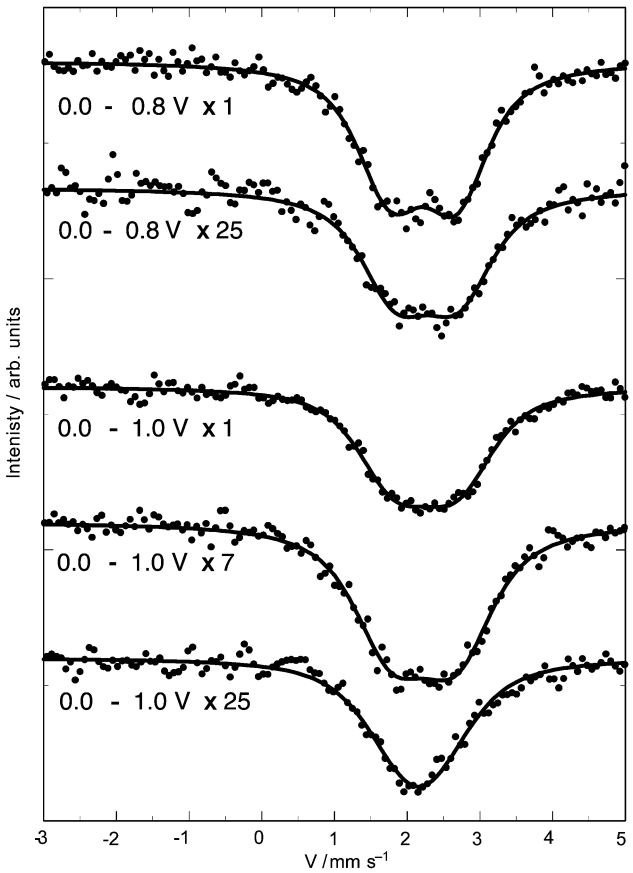

Fig. 6 Mössbauer spectra of cells recorded at 0.8 V and 1.0 V for increasing number of cycles.

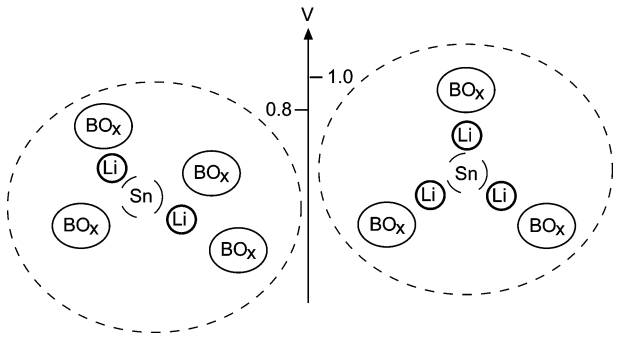

Fig. 7 Schematic picture of the local Sn environment in the glass electrode during the charging process after 25 cycles at the two different potentials.

For comparison, Mössbauer measurements were also performed on a cell made with another tin borate glass, $Sn_2B_3O_{6.5}$. Spectra of the cell were recorded before cycling, at the fully discharged state and after recharge to 1.5 V, see Fig. 8. From the figure it can be seen that the overall behaviour is similar to what was discerned for the SnB_2O_4 cell. Although the glass network structure differs slightly for the two glasses, the lithium ion insertion/extraction seems to affect tin in largely the same way.

Voltage range dependence on cycling performance

There is an obvious difference between cycling stability when comparing the two potential ranges, see Fig. 1. The (0.01–0.8) V cell clearly shows a superior insertion capability over the (0.01–1.0) V cell after 25 cycles. From the FT-IR measurements it can be discerned that the major effect of the lithium ion insertion/extraction on the glass network occurs during the first cycle, and the network is then very little affected by further cycling. Also the two voltage ranges show the same behaviour when comparing their DR-IR spectra, thus the stability of the glass network is almost unaffected by the voltage range. There are no differences in the Mössbauer spectra for the two voltage ranges after 7 cycles, in agreement with the cycling curve in which an equivalent cycling performance can be seen at that stage. A more lithium-rich tin environment was, however, found for the cell cycled up to 1.0 V after 25 cycles. This could therefore be an explanation for the decreasing capacity in this voltage range, as some lithium ions seem to be irreversibly trapped on cycling.

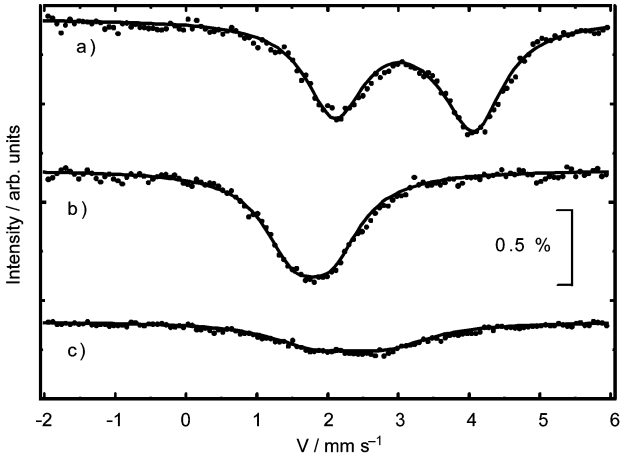

Fig. 8 Mössbauer spectra of a cell with $Sn_2B_3O_{6.5}$ as anode. a) Before cycling, b) fully discharged state and c) recharged to 1.5 V.

Conclusions

The network of the SnB_2O_4 glass is found to have some influence on the cycling stability. There is some disruption to the glass network during the first electrochemical cycle where mainly pyroborate and some orthoborate groups are formed. This disruption is responsible for a major part of the large capacity loss that only takes place during the first cycle. Except for the first cycle, when cycled below 1.0 V, the glass network seems to experience mostly reversible changes throughout the lithium ion insertion/extraction process. The tin environment, on the other hand, experiences an increase of lithium ions in its immediate environment when charging up to 1.0 V during repeated cycling. There is also a change towards a more symmetric environment for the tin. This might, upon repetitive cycling, cause additional local ordering of network units, which can then lead to further disruption of the glass network. The build up of lithium ions around tin seems to prevent some of the lithium ion insertion and thereby explains part of the decrease in discharge capacity found in the (0.01–1.0) V range. When charging up to 0.8 V instead, there is no such ordering or increase of lithium ions in the tin environment and also the cycling stability is improved.

Acknowledgements

This work has been supported by grants from the Foundation for Environmental Strategic Research (MISTRA), the Swedish Research Council (VR), and the Nordic Energy Research Program (NERP).

References

1 Y. Idota, T. Kobota, A. Matsufuji, Y. Maekawa and T. Miyasaka, *Science*, 1997, **276**, 1395.
2 I. A. Courtney and J. R. Dahn, *J. Electrochem. Soc.*, 1997, **144**, 2943.
3 G. R. Goward, F. Leroux, W. P. Power, G. Ouvrard, W. Dmowski, T. Egami and L. F. Nazar, *Electrochem. Solid-State Lett.*, 1999, **2**, 367.
4 Y. W. Xiao, J. Y. Lee, A. S. Yu and Z. L. Liu, *J. Electrochem. Soc.*, 1999, **146**, 3623.
5 J. Y. Lee, Y. Xiao and Z. Liu, *Solid State Ionics*, 2000, **133**, 25.
6 G. R. Goward, L. F. Nazar and W. P. Power, *J. Mater. Chem.*, 2000, **10**, 1241.
7 C. Gejke, E. Zanghellini, L. Fransson, K. Edström and L. Börjesson, *J. Phys. Chem. Solids*, 2001, **62**, 1213.
8 C. Gejke, E. Zanghellini, L. Fransson, K. Edström and L. Börjesson, *J. Power Sources*, 2001, **97-98**, 226.
9 I. A. Courtney, R. A. Dunlap and J. R. Dahn, *Electrochim. Acta*, 1999, **45**, 51.
10 S. Machill, T. Shodai, Y. Sakurai and J. Yamaki, *J. Solid State Electrochem.*, 1999, **3**, 97.
11 A. N. Mansour, S. Mukerjee, X. Q. Yang and J. McBreen, *J. Electrochem. Soc.*, 2000, **147**, 869.
12 K. Furuya, K. Ogawa, Y. Mineo, A. Matsufuji, J. Okuda and T. Erata, *J. Phys.: Condens. Matter*, 2001, **13**, 3519.
13 P. Kubelka and F. Munk, *Z. Tech. Phys.*, 1931, **12**, 593.
14 K. S. Kim and P. J. Bray, *J. Nonmet.*, 1974, **2**, 95.
15 S. A. Feller, W. J. Dell and P. J. Bray, *J. Non-Cryst. Solids*, 1982, **51**, 21.
16 E. I. Kamitsos, M. A. Karakassides and G. D. Chryssikos, *Phys. Chem. Glasses*, 1987, **28**, 203.
17 A. Paul, J. D. Donaldson, M. T. Donoghue and M. J. K. Thomas, *Phys. Chem. Glasses*, 1977, **18**, 125.
18 V. I. Goldanskii, G. M. Gorodinski, S. V. Karyagin, L. A. Korytko, L. M. Krizhanskii, E. F. Makarov, I. P. Suzdalev and V. V. Khrapov, *Proc. Acad. Sci. USSR, Phys. Chem. Sect.*, 1963, **147**, 766.
19 T. Ericsson and R. Wäppling, *J. Phys.*, 1976, **C6**, 719.
20 E. Nordström, S. Sharma, E. Sjöstedt, L. Fransson, L. Häggström, L. Nordström and K. Edström, *Hyperfine Interact.*, 2002, in press.
21 J. G. Stevens and W. L. Gettys, *Isomer Shift Reference Scales*, Mössbauer Effect Data Center, University of North Carolina, Asheville, NC, 1981.
22 J. K. Lees and P. A. Flinn, *J. Chem. Phys.*, 1968, **48**, 882.
23 J. Isidorsson, C. G. Granqvist, L. Häggström and E. Nordström, *J. Appl. Phys.*, 1996, **80**, 2367.
24 R. A. Dunlap, D. A. Small, D. D. MacNeil, M. N. Obrovac and J. R. Dahn, *J. Alloys Compd.*, 1999, **289**, 135.
25 J. Chouvin, J. Olivier-Fourcade, J. C. Jumas, B. Simon and O. Godiveau, *Chem. Phys.Lett.*, 1999, **308**, 413.